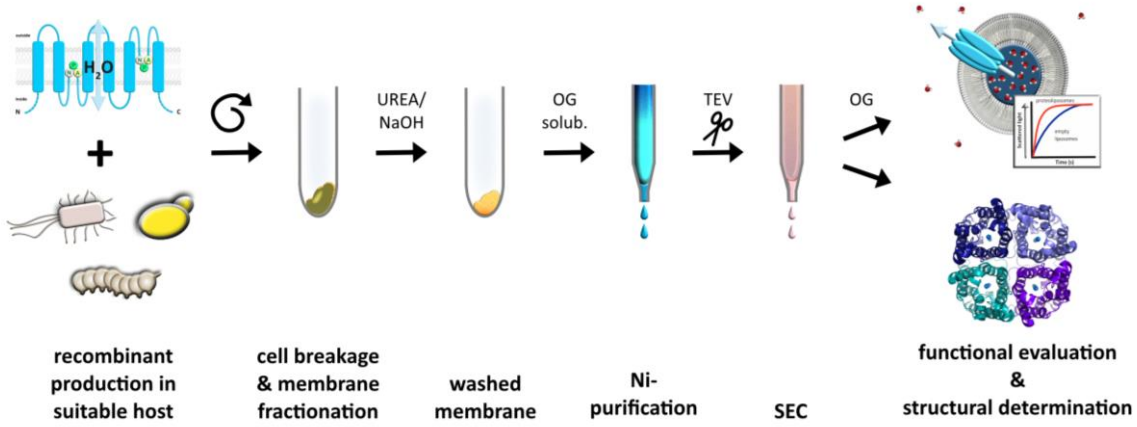
UREA/
NaOH
OG
solub.
TEV
OG
recombinant
production in
suitable host
cell breakage
& membrane
fractionation
washed
membrane
Ni-
purification
SEC
functional evaluation
&
structural determination

Aquaporins – expression, purification and characterization

Roslyn M. Bill[1] & Kristina Hedfalk[2]

[1] College of Health and Life Sciences, Aston University, Aston Triangle, Birmingham B4 7ET, UK

[2] Department of Chemistry and Molecular Biology, Gothenburg University, Box 462, 405 30 Göteborg, Sweden

Running title: Aquaporin production

Corresponding author: Kristina Hedfalk, Department of Chemistry and Molecular Biology, Gothenburg University, Box 463, 405 30 Göteborg, Sweden, +46-31-786 3923, kristina.hedfalk@gu.se

Keywords

Aquaporin, water channel, recombinant production, proteoliposomes,

Highlights

- Aquaporins are integral membrane proteins where dysfunction in the water transport connects to a broad spectra of diseases and cellular disorders
- The majority of the aquaporin isoforms can be produced by recombinant protein production
- High yields of stable protein are routinely achieved after a two-step purification procedure using common detergents

Abstract

Aquaporin water channels facilitate the bi-directional flow of water and small, neutral solutes down an osmotic gradient in all kingdoms of life. Over the last two decades, the availability of high-quality protein has underpinned progress in the structural and functional characterization of these water channels. In particular, recombinant protein technology has guaranteed the supply of aquaporin samples that were of sufficient quality and quantity for further study. Here we review the features of successful expression, purification and characterization strategies that have underpinned these successes and that will drive further breakthroughs in the field. Overall, *Escherichia coli* is a suitable host for prokaryotic isoforms, while *Pichia pastoris* is the most commonly-used recombinant host for eukaryotic variants. Generally, a two-step purification procedure is suitable after solubilization in glucopyranosides and most structures are determined by X-ray following crystallization.

1. Introduction

Water is essential for life and is the major component of all organisms. Aquaporin water channels facilitate the bi-directional flow of water (and, in some cases, small, neutral solutes such as glycerol and urea, as well as gases like carbon dioxide and ammonia) down an osmotic gradient in all cells [1]. In addition, some aquaporin isoforms play a role as peroxiporins, contributing to cellular redox signaling by transferring hydrogen peroxide [2]. The thirteen aquaporins that are found throughout the human body facilitate the secretion of body fluids like cerebrospinal fluid, tears, saliva, sweat and bile, and the concentration of urine [3]. Aquaporins are involved in diverse and common clinical disorders including loss of vision, loss of skin barrier function, kidney diseases, the brain oedema that follows stroke or head trauma [4] and also in various pathophysiological conditions including Alzheimer's and Parkinson's [5, 6]. Furthermore, aquaporins have multiple functions in plants such as controlling the hydraulics of plant tissue as well as seed germination and the emergence of lateral roots [7]. Plants with genetically altered aquaporins may also have improved tolerance to stresses such as drought [8]. Furthermore, the presence of aquaporins has been suggested to enable microorganisms to have specific lifestyles. For example, aquaporins enhance cellular tolerance against rapid freezing, suggesting their ecological relevance [9]. Based on these examples, it is clear that the understanding of aquaporin structure and function is essential to address fundamental questions in health and disease in all kingdoms of life.

It is now 20 years since the first high-resolution structure of an aquaporin was reported for hAQP1, which was determined to 3.8 Å by electron diffraction (ED) [10] using protein extracted from its native source, the membranes of human red blood cells [11]. The reporting of new aquaporin structures has continued steadily since then meaning that in December 2020, there were 31 aquaporin structures in total from both eukaryotes and prokaryotes. The

majority of these high-resolution structures (74%) have been derived by X-ray crystallography, a substantial fraction (23%) by ED and one by NMR **(**https://blanco.biomol.uci.edu/mpstruc/; **Table 1)**. Of the 13 human aquaporins, six isoforms have a high resolution structure; AQP1 [10, 12-14], AQP2 [15, 16], AQP4 [17], AQP5 [18], AQP7 [19] and AQP10 [20]. In addition, AQP1 [21] and AQP4 [22, 23], as well as AQP0 [24-27], have structures where the protein has been derived from other mammalian sources (rat, cattle and sheep). Two plant plasma membrane intrinsic protein (PIP) isoforms have had their structures determined, SoPIP2;1 [28] from spinach and AtPIP2;4 [29] from *Arabidopsis thaliana*, as well as one tonoplast intrinsic protein (TIP) isoform, AtTIP2;1 [30] from *A. thaliana*. Eukaryotic microorganims are represented by the structure of yeast Aqy1 [31, 32] and there is a structure from the unicellular protozoan, *Plasmodium falciparum*, PfAQP [33]. Finally, there are three high resolution structures of prokaryotic aquaporins, AqpM [34], AqpZ [35-38] and GlpF [39, 40].

As a result of this progress, the size and shape of aquaporins pores are understood in precise atomic detail. This has enabled a molecular-level understanding of how aquaporins allow water molecules (but not protons) to permeate cell membranes (**Fig. 1**). Aquaporins assemble as homotetramers where each monomer forms an individual channel [41]. The very first low resolution hAQP1 structure (determined to 6 Å by ED [42]), revealed the ‘hour-glass model’ where the two NPA-containing loops dip into the membrane from either side forming the center of the aqueous pore [43]. When the resolution was improved to to 2.2 Å, the mechanism for proton exclusion could be deduced as involving the NPA motifs for interrupting a continues chain of water through the aqueous pore [21]. The first high resolution structure of a glycerol channel, GlpF from *Escherichia coli*, provided insight into a constriction region (commonly referred to as the ar/R region) towards the external entrance of

the channel as the determinant of channel selectivity [39]. More recent insights into aquaporin specificity are provided by the structure of AtTIP2;1, which can transport ammonia [30]. AtPIP2;4 can transport hydrogen peroxide [29], but a very high resolution structure will be required in order to understand the mechanism of permeation due to its high similarity with water. High resolution aquaporin structures have additionally provided novel insights into the regulation of water flow by pH, phosphorylation and mechanosensitivity [20, 28, 32, 44, 45].

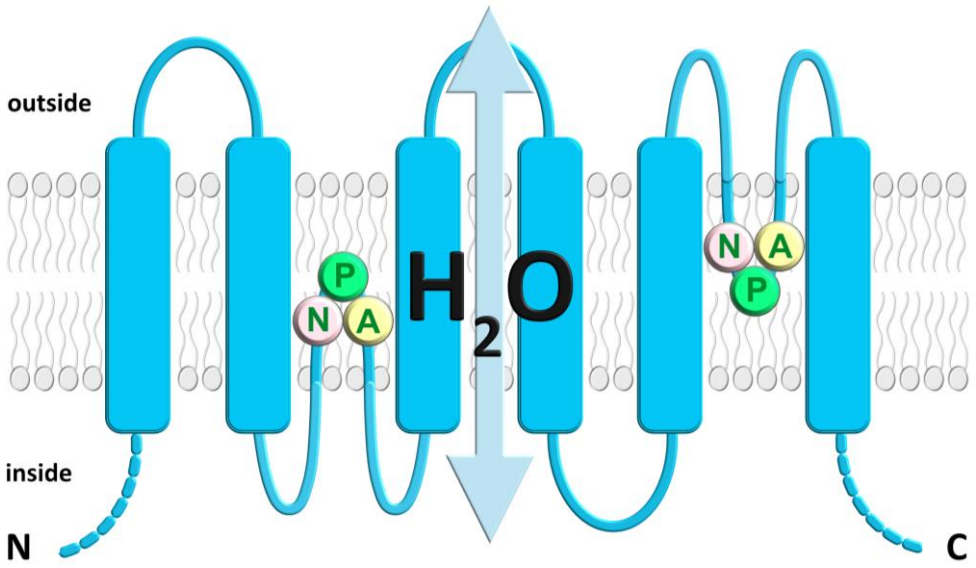

Figure 1. Aquaporin topology. All aquaporins share a common topology of six transmembrane α-helices and five connecting loops. The second and fifth loops contain the family's highly-conserved, signature NPA motifs that meet at the center of the membrane in the three dimensional fold forming a selectivity filter for bidirectional water flow excluding protons. The N-and the C-termini are cytosolic and vary in length among aquaporin homologues (as indicated by dashed lines), are often binding sites for interacting proteins and provide regulatory motifs.

Human aquaporins have been assumed to be constitutively expressed in membranes [46], meaning that any rapid changes in membrane water permeation could only be passively facilitated by changes to local osmotic gradients. This view is inconsistent with the need for

cellular water flow to rapidly change in response to constantly-fluctuating extracellular environments [47]. Control *via* gene expression can alter water permeability in the long-term, but is too slow for a rapid response. Instead, conformational changes of individual aquaporin pores (‘gating’, observed in plant and microbial aquaporins) or regulating the number of pores by moving them to and from the membrane (more pores resulting in higher water permeability) are candidate mechanisms [44, 48]. One of the most well-established mechanisms of regulation by translocation is the permeability of kidney cell membranes being a function of AQP2 membrane abundance, which changes in response to the anti-diuretic hormone, vasopressin [49]. This is often seen as an idiosyncrasy even though hormones may control the localization of other human AQPs [46]. Additional examples of translocation come from our recent work that has challenged the assumption of constitutive expression, showing that subcellular relocalization in response to non-hormonal signals is a regulatory mechanism controlling human AQP1 [50, 51], AQP4 [52-54] and AQP5 [55]. These examples illustrate that a future challenge will be to characterise the molecular mechanisms of aquaporin regulation *in vitro* and *in vivo*, which is now essential to understand the physiological control of water homeostasis.

The availability of high-quality protein that has underpinned progress in aquaporin structural biology is now required to address many of the remaining open questions about aquaporin regulation. In this review, we analyse how aquaporin protein samples have been prepared for structural biology. These approaches have guaranteed the supply of samples that are of sufficient quality and quantity for further study and that will underpin further functional studies in the field. Access to recombinant material will aid the progress of structural determination since it allows protein engineering to improve stability of the protein target and also the isolation of isoforms, critical aspects that are limitations of working with the native

source. The scope of this review is to summarize the experimental approaches that have enabled structural analysis of aquaporin homologues to high resolution, specifically the details of their expression, purification and functional characterization.

Table 1. Aquaporin structures determined to high resolution (<4Å resolution). Aquaporin structures derived from recombinant protein production in heterologous hosts are shaded in grey and those derived from recombinant production using the homologues host are highlighted in pale yellow. Entries without shading are derived from protein extracted from native cells or tissues.

Target	Source	Host	Method	Resolution	PDB Code	Ref
EUKARYOTIC						
Mammalian						
AQP0	*Bos taurus*	-	X-ray	2.24 Å	1YMG	Harries et al. (2004)
AQP0	*Ovis aries*	-	ED	3.0 Å	1SOR	Gonen et al. (2004)
AQP0	*Ovis aries*	-	ED	1.9 Å	2B6O	Gonen et al. (2005)
AQP0	*Ovis aries*	-	ED	2.5 Å	3M9I	Hite et al. (2010)
AQP1	*Homo sapiens*	-	ED	3.8 Å	1FQY	Murata et al. (2000)
AQP1	*Homo sapiens*	-	ED	3.7 Å	1IH5	Ren et al. (2001)
AQP1	*Homo sapiens*	*S. frugiperda*	X-ray	3.28 Å	4CSK	Ruiz Carrillo et al. (2014)
AQP1	*Homo sapiens*	*P. pastoris*	NMR	-	6POJ	Dingwell et al. (2019)
AQP1	*Bos taurus*	-	X-ray	2.20 Å	IJ4N	Sui et al. (2001)
AQP2	*Homo sapiens*	*P. pastoris*	X-ray	2.75 Å	4NEF	Frick et al. (2014)
AQP2	*Homo sapiens*	*P. pastoris*	X-ray	3.7 Å	6QF5	Lieske et al. (2019)
AQP4	*Rattus norvegicus*	*S. frugiperda*	ED	3.2 Å	2D57	Hiroaki et al. (2005)
AQP4	*Rattus norvegicus*	*S. frugiperda*	ED	2.8 Å	2ZZ9	Tani et al. (2009)
AQP4	*Homo sapiens*	*P. pastoris*	X-ray	1.8 Å	3GD8	Ho et al. (2009)
AQP5	*Homo sapiens*	*P. pastoris*	X-ray	2.0 Å	3D9S	Horsefield et al. (2008)
AQP7	*Homo sapiens*	*P. pastoris*	X-ray	1.9 Å	6QZI	de Maré et al. (2020)
AQP10	*Homo sapiens*	*S. cerevisiae*	X-ray	2.3 Å	6F7H	Gotfryd et al. (2018)
Plant						
PIP2;1	*Spinacia oleracea*	*P. pastoris*	X-ray	2.1 Å	1Z98	Törnroth-Horsefield et al. (2006)
PIP2;1	*Spinacia oleracea*	*P. pastoris*	X-ray	2.3 Å	3CLL	Nyblom et al. (2009)
PIP2;4	*Arabidopsis thaliana*	*P. pastoris*	X-ray	3.7 Å	6QIM	Wang et al. (2019)
TIP2;1	*Arabidopsis thaliana*	*P. pastoris*	X-ray	1.18 Å	5I32	Kirscht et al. (2016)
Eukaryotic microorganism						
PfAQP	*Plasmodium falciparum*	*E. coli*	X-ray	2.05 Å	3C02	Newby et al. (2008)
Yeast						
Aqy1	*P. pastoris*	-	X-ray	1.15 Å	2W2E	Fischer et al. (2009)
Aqy1	*P. pastoris*	-	X-ray	0.88 Å	3ZOJ	Kosinska Eriksson et al. (2013)
PROKARYOTIC						
Methanothermobacter marburgensis						
AqpM	*M. marburgensis*	*E. coli*	X-ray	1.68 Å	2F2B	Lee et al. (2005)
Escherichia coli						
AqpZ	*E. coli*	*E. coli*	X-ray	2.5 Å	1RC2	Savage et al. (2003)
AqpZ	*E. coli*	*E. coli*	X-ray	3.2 Å	2ABM	Jiang et al. (2006)
AqpZ	*E. coli*	*E. coli*	X-ray	2.3 Å	2O9D	Savage & Stroud (2007)
AqpZ	*E. coli*	*E. coli*	X-ray	2.4 Å	3NK5	Savage et al. (2010)
GlpF	*E. coli*	*E. coli*	X-ray	2.2 Å	1FX8	Fu et al. (2000)
GlpF	*E. coli*	*E. coli*	X-ray	2.1 Å	1LD5	Tajkhorshid et al. (2002)

2. Aquaporin production and characterization

2.1 The majority of aquaporin structures have human origin

Of the structures shown in Table 1, 24 have eukaryotic origin (17 mammalian, four plant, one eukaryotic microorganism, and two yeast) and seven have prokaryotic origin (one *M. marburgensis* and six *E. coli*) **(Fig. 2A)**. Among the total number of aquaporin structures, about 50% (15) are unique proteins and for several isoforms there are multiple examples of structures of the same protein, generally with an increase in resolution over time **(Table 1)**. Also worth noting, is that the majority of structures are derived from mammals and nearly 60% (10/17) of those are recombinantly produced. Of the mammalian aquaporins, six of the 13 human isoforms are represented by eight structures, being the most common source (26%) of all aquaporin structures. Furthermore, there is a clear dominance of crystallization and X-ray diffraction as method for high resolution structural characterization, while ED has been a successful method for early structures of AQP0 [24, 25, 27] and hAQP1 [10, 13], and also for AQP4 [22, 23].

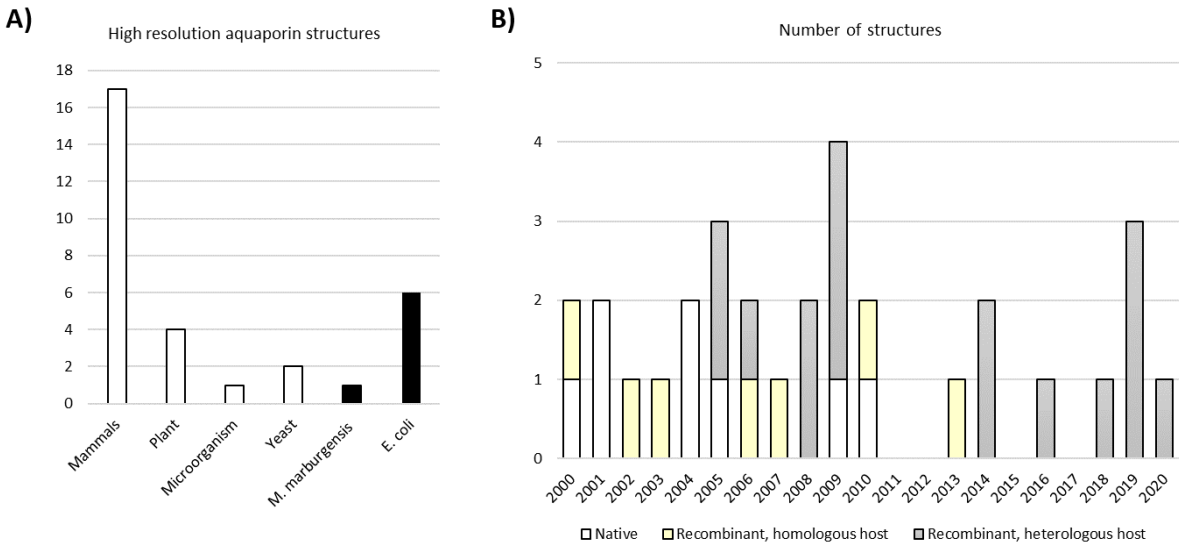

Figure 2. Origin of aquaporin protein samples used for structural determination 2000-2020. A) All kingdoms of life are represented; mammals, plant, microorganism, yeast, and bacteria. Eukaryotic targets are

shown in white bars and prokaryotic targets are shown in black bars, as listed in **Table 1**. B) For the first eight years, structures of protein derived from the native source dominated, while for the last twelve years, almost all aquaporin structures relied on recombinant heterologous production.

2.2 **Pichia pastoris** *is the most common host for recombinant production*

Initially, all aquaporin structures were derived from their native source but with time, recombinant protein production has become the dominant source of protein for aquaporin structural biology **(Fig. 2B)**. More precisely, until 2004, only structures from proteins extracted from their native source or recombinant bacterial aquaporins produced in their homologous host were solved. In 2005 two ED structures were reported that were derived from recombinant production using heterologous hosts; AQP4 from *Rattus norvegicus* produced in *S. frugiperdam* [22] and AqpM from *M. marburgensis* produced in *E. coli* [34]. Since 2009, all aquaporin structures but one have been derived from recombinant protein production, the exception being Aqy1 extracted from the native membrane of the yeast *Pichia pastoris* (also known as *K. phaffii* and *K. pastoris* [56]) [32].

Looking at the 24 eukaryotic aquaporin structures, the majority of those (63%) are produced recombinantly. Of the 15 structures produced using a host different from the native source, the vast majority (73%) were produced in yeast; *S. cerevisiae* or *P. pastoris*, where hAQP10 is the only aquaporin structure of protein produced in *S. cerevisiae* [20] **(Table 1)**. Furthermore, there is only one example of a successful production of a eukaryoic aquaporin in *E. coli*, and that is the PfAQP from the malaria parasite *P. falciparum* [33]. It is also worth noting that insect cells, *S. frugiperda*, are not commonly used to produce aquaporins, hAQP1 [14] and AQP4 from rat [22, 23] being the only proteins produced in this host. In comparison, three prokaryotic aquaporin structures have been determined, those of AqpM [34], AqpZ [35-38] and GlpF [39, 40] **(Table 1)**. All those proteins are produced recombinantly in *E. coli*, which is the homologues host for AqpZ and GlpF.

2.3 Inclusion of polyhistidine tags and truncated termini are common features guiding expression construct design

The actual construct design is of utmost importance for successful recombinant production of a membrane protein target commonly using a heterologous host. Taking a closer look at the 23 recombinant aquaporins for which a structure has been determined, all but two, Aqy1 [31] and SoPIP2;1 [28] are produced with a polyhistidine tag for purification, also enabling detection by immunoblot **(Table 2)**. The length of the polyhistidine tag typically varies between six and ten residues, and for eukaryotic targets, there is no real preference in the location at the N- or C-terminus. In contrast, for prokaryotic targets only N-terminal polyhistidine tags have been used, with six residues being the most common length. In the design of aquaporin constructs, a protease cleavage site is always introduced after the N-terminal polyhistidine-tag while this is seldom the case for C-terminal fusions, PIP2;4 from *A. thaliana* being the only exception [29] **(Fig. 3A)**. Furthermore, truncations of hydrophilic extensions are common in the construct design in order to remove flexible domains that might disrupt crystal packing. For aquaporin structures, however, that approach is relatively uncommon having been used in just five of the 16 recombinant eukaryotic proteins representing three aquaporin isoforms; hAQP2 [15, 16], hAQP7 [19], hAQP10 [20] and AtPIP2;4 [29]. Codon optimization is another engineering approach that has been applied for four euakryotic aquaporin targets; hAQP2 [15], hAQP10 [20] and AtPIP2;4 [29] produced in yeast as well PfAQP [33] produced in *E. coli* **(Table 1 and 2)**.

Table 2. Protein engineering approaches for recombinant production of aquaporins.

Target	His-tag	terminus	cleavage site	trunc	codon opt	Ref
EUKARYOTIC						
Mammalian						
AQP1	6x	N	TEV	-	-	Ruiz Carrillo et al. (2014)
AQP1	6x	C	-	-	-	Dingwell et al. (2019)
AQP2	8x	N	TEV	yes	yes	Frick et al. (2014), Lieske et al. (2019)
AQP4	6x	C	-	-	-	Hiroaki et al. (2005)
AQP4	6x	C	-	-	-	Werten et al. (2001)
AQP4	8x	N	3C	-	-	Ho et al. (2009)
AQP5	6x	C	-	-	-	Horsefield et al. (2008)
AQP7	6x	C	-	yes		de Maré et al. (2020)
AQP10	8x	C	-	yes	yes	Gotfryd et al. (2018)
Plant						
PIP2;1	6x	C	-	-	-	Törnroth-Horsefield et al. (2006)
PIP2;1	6x	N	Throm	-	-	Nyblom et al. (2009)
PIP2;4	8x	C	TEV	yes	yes	Wang et al. (2019)
TIP2;1	10x	N	TEV	-	-	Kirscht et al. (2016), Karlsson et al. (2003)
Eukaryotic microorganism						
PfAQP	6x	N	Throm	-	yes	Newby et al. (2008)
Yeast						
Aqy1	-	-	-	-	-	Kosinska Eriksson et al. (2013)
PROKARYOTIC						
Methanothermobacter marburgensis						
AqpM	10x	N	FacXa	-	-	Kozono et al. (2003), Lee et al. (2005)
Escherichia coli						
AqpZ	6x	N	Tryps	-	-	Savage et al. (2003), Borgnia et al. (1999)
AqpZ	yes	N	Throm	-	-	Jiang et al. (2006), Daniels et al. (2004)
AqpZ	6x	N	Tryps	-	-	Savage et al. (2003), Savage & Stroud (2007)
AqpZ	6x	N	Tryps	-	-	Savage et al. (2003), Savage et al. (2010)
GlpF	6x	N	Throm	-	-	Fu et al. (2000)
GlpF	6x	N	Throm	-	-	Fu et al. (2000)

2.4 Aquaporins are stable in glucopyranosides

Solubilization of the integral membrane protein is a critical first step in the purification process where high efficiency and retained function have to be taken into consideration. For aquaporins, an initial membrane wash is an additional common step preceding the actual solubilization having the benefit of enriching the yield of integral membrane proteins, including the aquaporins, commonly leading to a higher efficiency in the solubilization step. The tradition of stripping the membrane from peripheral proteins loosely attached to the surface originates from the purification of AQP1 from blood, where 1 M KI was used for the early purifications of hAQP1 from red cell membrane vesicles [11]. For eukaryotic aquaporins recombinantly produced in various hosts, a urea wash (typically 4M) sometimes followed by a NaOH wash (typically 20 mM), is the common procedure. This protocol for urea/alkali stripping of the membrane was presented as a crucial step in the purification of PM28A (latter called SoPIP2;1) from spinach leaf plasma membranes having dual benefits; non-membrane protein contaminants were reduced and the lipid bilayer was more accessible for the solubilizing detergent [57]. This wash is applied in most cases, with the exceptions of recombinant hAQP1 [12, 14], hAQP4 [17], hAQP10 [20] and PfAQP [33], and there is no correlation between membrane wash and the host system used **(Table 3)**. When it comes to detergents used for solubilization, there is a clear dominance for n-octyl-β-D-glucopyranoside (OG) which was used for nearly 70% of the 31 aquaporins from which a high resolution structure is derived **(Fig. 3B)**, and here all the prokaryotic isoforms are included. Thus, aquaporins are apparently stable in glucopyranosides, OG as well as its relative n-nonyl β-D-glucopyranoside (NG), and the more mild long chain detergents, (n-decyl- β-maltoside) DM and (n-dodecyl- β-maltoside) DDM, are only used in a few cases; native hAQP0 [24, 25] as well as recombinant hAQP7 [19] and hAQP10 [20]. There are also a few cases using more unusual detergents for solubilization, like Triton X-100 for native hAQP1 [10] and

lauryldimethylamine oxide (LDAO) for AtPIP2;4 [29]. Taken together, aquaporins are seemingly robust integral membrane proteins that can tolerate both membrane wash and rather harsh treatment for solubilzation without losing their fold and function. The same is true for the detergent choice for the subsequent purification and preparation for structural determination, OG is by far the most common detergent and the long chain detergents DM and DDM are rather uncommon **(Fig. 3C)**. The main difference compared to the solubilization step is that octyl glucose neopentyl glycol (OGNPG) are used to some extent, for crystallization of recombinant hAQP2 [15, 16] and hAQP7 [19]. In conclusion, some detergents are only used for solubilization, although uncommon (TX-100 and LDAO), and a detergent exchange is performed for preparation of crystals, while OGNPG detergents is solely used for crystallization (OGNPG) **(Table 3)**.

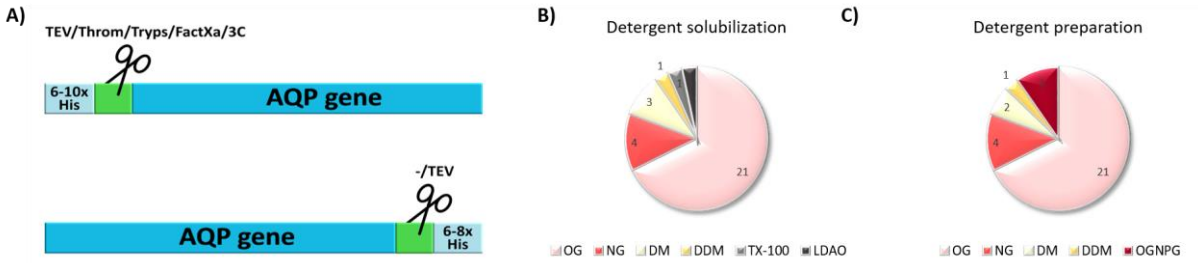

Figure 3. Construct design for recombinant production of aquaporins and detergents used for aquaporin purification. A) Most aquaporins are produced in fusion with a polyhistidine tag at the N- or C-terminus to assist purification and immunodetection. The length of the polyhistidine tag typically varies between six and ten residues. For N-terminal polyhistidine tags, a cleavage site is always inserted before the gene sequence while this is most often not the case for C-terminal tags. B) Detergents used for solubilization of aquaporins. C) Detergents used in the preparation of aquaporins for structural determination using crystallization and X-ray, ED or NMR.

2.5 The use of Ni-NTA purification and cleavable polyhistidine tags is the most common purification approach

As already described in section 2.3, a polyhistidine tag is most commonly introduced in the construct design for aquaporin recombinant production, in fact as many as 22 of the 31 (71%) aquaporin structures are derived from such constructs where an N-terminal polyhistidine tag is most commonly cleaved of using a protease cleavage site **(Fig. 3A)**. This means that affinity purification is the most typical purification method for aquaporins using Ni-NTA chromatography with a pH ranging from 7 to 8, there is only one case, AqpM [34], using Co^{2+}-Sepharose instead **(Table 3)**. For those aquaporins that are purified from their native source, ion exchange is the most common first purification step, a method that has also been used for aquaporins recombinantly produced to high yields in their native form in *P. pastoris*; hAQP5 [18], SoPIP2;1 [28] and Aqy1 [32]. Anion exchange using a pH between 7.5 and 8 is slightly more common than cation exchange, where a more wide range of pH is applied, 6 to 9. There are two exceptions from the more common procedures for aquaporin purification, and that is using phenylboronic acid-agarose (PBA) affinity chromatography as a preceding step to anion exchange chromatography for hAQP1 extracted from erythrocytes and an *Erythrina cristagalli* lectin chromatography after, with the purpose to isolate differently glycosylated forms of the protein [58]. Independent of the method used for the first purification step, the utmost majority of purification procedures include a second purification step consisting of Size-Exclusion Chromatography (SEC) using a pH range of 6-8 before preparation for structural determination. There are only three exceptions from this where only one purification step is applied; native hAQP1 for ED [11], recombinant hAQP1 for NMR [12] as well as AQP4 from rat for ED [22] **(Table 3)**.

Reflecting on the final yield from the various purifications, it is noteworthy that this information is commonly lacking. The final concentration for preparation of the protein

solution for crystal determination is the more frequent information. This is an interesting notion since a high yield of homogenous protein material is an absolute requirement for succeeding with structural characterization, mostly pronounced for crystallization approaches which most often requires numerous rounds of trial and error. However, in 35% of the cases the yield is clearly reported, most often as mg/L, ranging from 0.2-25 mg/L, and in a few cases as mg/g cells, ranging from 0,3-1.1 mg/g **(Table 3)**.

Table 3. Protein purification of aquaporins for structural determination.

Target	Membrane wash	Detergent solubilzation	Purification 1st step	Purification 2nd step	Yield	Detergent analysis	Ref
EUKARYOTIC							
Mammalian							
AQP0	-	OG	C-IEX[3] pH 9	SEC pH 7	N/A	NG	[26]
AQP0	-	DM	A-IEX[4] pH 8	SEC pH 8	N/A	DM	[24]
AQP0	-	OG	A-IEX pH 8	SEC pH 8	N/A	OG	[27]
AQP1	KI[1]	TX-100	A-IEX pH 7.8	-	N/A	OG	[10, 11]
AQP1	-	OG	PBA[5], A-IEX, lectin[6]	SEC	N/A	OG	[13, 58]
AQP1	-	OG	Ni-NTA[7] pH 8	SEC pH 8	1-3 mg/L	DDM	[14]
AQP1	-	OG	Ni-NTA pH 8	-	N/A	OG	[12]
AQP1	N-laurylsarcosine	NG	A-IEX pH 7.5	SEC	N/A	NG	[21]
AQP2	urea	NG	Ni-NTA pH 8	SEC pH 8	N/A	OGNPG	[15]
AQP4	urea, alkali[2]	OG	Ni-NTA pH 7	-	3 mg/L	OG	[22]
AQP4	urea, alkali	OG	Ni-NTA pH 8	SEC pH 8	N/A	OG	[23, 59]
AQP4	-	OG	Ni-NTA pH 7.4	SEC pH 6.0	15 mg/l	OG	[17]
AQP5	urea, alkali	NG	C-IEX pH 6	SEC pH 7.5	N/A	NG	[18]
AQP7	alkali	DDM	Ni-NTA pH 8	SEC pH 7.5	N/A	OGNPG	[19]
AQP10	-	DM	Ni-NTA pH 7.5	SEC pH 8	N/A	NG	[20]
Plant							
PIP2;1	urea/alkali	OG	Ni-NTA pH 7.5/C-IEX pH 7.0	SEC pH 7.5	N/A	OG	[28]
PIP2;1	urea, alkali	OG	C-IEX pH 7.0	SEC pH 7.5	25 mg/L	OG	[60]
PIP2;4	urea	LDAO	Ni-NTA pH 8	SEC pH 8	0,5 mg/g cells	OG	[29]
TIP2;1	urea	OG	Ni-NTA pH 7.8	SEC pH 7.8	1,1 mg/g cells	OG	[30, 61]
eukaryotic microorganism							
PfAQP	-	OG	Ni-NTA pH 7.4	SEC pH 7.4	0,2 mg/L	OG	[33]
yeast							
Aqy1	urea, alkali	OG	A-IEX pH 8	SEC pH 8	N/A	OG	[32, 62]
Aqy1	alkali	OG	A-IEX pH 8	SEC pH 8	N/A	OG	[31, 32, 62]
PROKARYOTIC							
Methanothermobacter marburgensis							
AqpM	-	OG	Co-Seph[8] pH 7.4	SEC pH 7.4	4 mg/L	OG	[34]
Escherichia coli							
AqpZ	-	OG	Ni-NTA pH 7.4	SEC pH 6.0	2,5 mg/L	OG	[36, 63]
AqpZ	-	OG	Ni-NTA pH 7.5	SEC pH 7.0	12 mg/L	OG	[35, 64]
AqpZ	-	OG	Ni-NTA pH 7.4	SEC pH 7.4	10 mg/L	OG	[36, 38]
GlpF		OG	Ni-NTA	SEC	N/A	OG	[39, 40]

[1]KI, potassium iodide; [2]alkali, typically 20 mM NaOH (pH~12) [3]C-IEX, cation ion exchange chromatography; [4]A-IEX, anion ion exchange chromatography; [5]PBA, phenylboronic acid-agarose affinity chromatography; [6]lectin, Erythrina cristagalli lectin chromatography; [7]Ni-NTA, immobilized metal affinity chromatography using nickel nitrilotriacetic acid; [8]Co-Seph, immobilized metal affinity chromatography using cobolt sepharose

2.6 Proteoliposome studies combined with molecular dynamics simulations is the standardized characterization method

The most typical way to evaluate the function of purified aquaporins is to reconstitute the protein into liposomes. Using a stopped flow spectrophotometer, the proteoliposomes are quickly mixed with a high osmolarity solution and, as a consequence, the proteoliposomes will shrink faster than the control liposomes due to a more efficient water flow via the aquaporins **(Fig. 4)**, a method that was first established for CHIP28, later named hAQP1 [65]. Of the 31 aquaporins having a high resolution structure **(Table 1)**, 17 (>50%) were functionally characterized using proteoliposomes. The shrinkage upon the sudden increase in external osmolarity is measured as scattered light at the wavelength around 438 nm and the fixed angle of 90°. Light scattering was used for all water flow measurements for the examples shown in **Table 1**, typically measured for 1 second. For increased sensitivity of the assay, proteoliposomes can be preloaded with carboxy-fluorescein (typically 0.5 mM) and the change in fluorescence is recorded at an excitation of 490 nm. The only example of the use of fluorescence is the measurement of ammonium transport evaluated for AtTIP2;1 [30]. Generally, *E. coli* Polar Lipid Extract is used to make liposomes for reconstitution of aquaporins, as exemplified by recombinant hAQP1 [62]. The effect of the lipid to protein ratio is sometimes analysed within the same study which gives rise to different water flow rates for a specific aquaporin isoform, as shown for recombinant AqpZ [63], hAQP5 [18] as well as SoPIP2;1 [61]. The osmotic gradient is commonly provided by high concentrations of sorbitol, around 300 mM [62]. But there are variations to this setup, exemplified by functional analysis of recombinant hAQP10 reconstituted in proteopolymersomes and an osmotic gradient provided by 0.5 M NaCl [20] as well as Aqy1, where *P. pastoris* spheroplasts were used to assay function [32]. The proteoliposome assay can also be used to evaluate flow of carbohydrates such as glycerol flow via GlpF [39]. The negative control constituted of empty

liposomes is most commonly included. Whenever applicable, the protein specific inhibition by mercury is also included, first identified as an inhibitor by binding to cysteine 189 in hAQP1 [66].

The resulting data are normally presented as the graph from the scattered light, where averaged curves from multiple mixing events are commonly shown. Frequently, the curves are fitted to a one or two exponential equation to estimate the rate constant for the initial event, presented with statistic, and sometimes the osmotic water permeability coefficient (P_f) is calculated where the size of the proteoliposomes are taken into account.

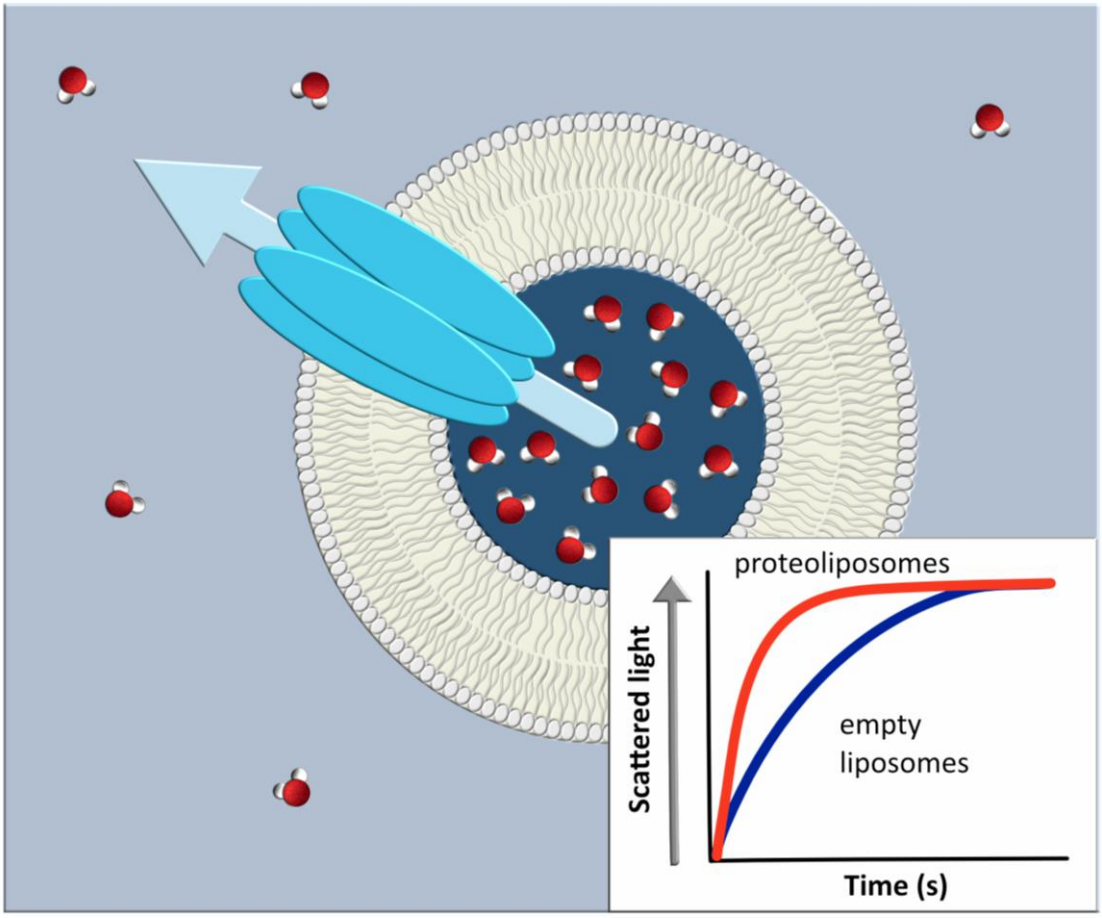

Figure 4. Functional analysis of aquaporins reconstituted in liposomes. Scattered light is measured upon shrinkage of the liposomes following an increase in external osmolarity.

Furthermore, structural and functional analyses are frequently accompanied by molecular dynamics (MD) simulations, which is the case for nearly 30% of the studies in **Table 1** (9/31). Simulations have assisted the understanding of how water flow excludes protons in the bacterial glycerol channel GlpF [40] and the water channel hAQP4 [17], and also illustrated the detailed movement of water molecules through the AQY1 channel at a resolution of 0.88 Å [31]. Specificity among different aquaporin isoforms has also been studied by MD to evaluate glycerol as well as ammonia flow in hAQP7 [19] and AtTIP2:1 [30], respectively. Furthermore, simulations have been involved in the analysis of aquaporin gating by pH in hAQP10 [20], by pH and phosphorylation in SoPIP2;1 [60] as well as by mechanosensitivity and phosphorylation in AQY1 [32]. To study the regulatory mechanism defined by phosphorylation, however, a multi-faceted approach is commonly needed in combination with structural analysis [44]. Taken together, MD and functional analysis using proteoliposomes is generally combined to support structural analysis, with three exceptions where MD has been used alone; hAQP7 [19] as well as follow up studies on GlpF [40] and AQY1 [31].

3. A consensus on aquaporin production emerges

Membrane proteins are well known challenging targets to study, mainly due to difficulties in extracting the high amount needed for structural efforts from the biological membrane, most pronounced for eukaryotic targets [67]. However, development of host systems combined with sophisticated engineering approaches has led to an increase in the number of high resolution structures, also for one of the most challenging protein families, the GPCRs (https://blanco.biomol.uci.edu/mpstruc/). The observed increase in eukaryotic structures goes hand in hand with the development of suitable eukaryotic production hosts, such as HEK293 cells and insect cells (*S. frugiperda*), but also yeast (*S. cerevisiae* and *P. pastoris*) [68]. For proteins from the GPCR family, for example, insect cells are more or less established as the recombinant production host of choice [69], while a simpler eukaryotic host, like yeast, has worked well for eukaryotic aquaporins. Indeed, there are examples of very high recombinant production of hAQP1 in both *S. cerevisiae* [70] and *P. pastoris* [62], where the latter is the basis for the only aquaporin NMR structure presented in **Table 1** [12]. Further comparisons with GPCRs show that more advanced engineering approaches were required to produce sufficiently stable proteins in high yields, including truncations, fusions, chimeras as well as stabilizing mutations [69], while a more simplistic approach has worked well for aquaporin constructs **(Fig. 3A)**. It is also worth noting that aquaporins commonly tolerate a harsh membrane wash, which provides a first enrichment step having the potential to make subsequent solubilization and purification more efficient, where short chain detergents (like OG and NG) are most frequently used throughout the whole process. Taken together, this illustrates that aquaporins in general constitute stable membrane proteins that, in comparison with more flexible and more challenging membrane protein targets like GPCRs, are rather straight forward targets for structural approaches (since protein stability is a key factor for success). However, this fact does not exclude the need for optimization efforts based on the

observation that homologues aquaporins are produced to different levels in yeast [71]. For codon-optimized sequences [72], certain homologues such as hAQP4 required substantial optimization of the genetic design in order to achieve high yields in *P. pastoris* [73]. Worth noting as well, is that codon optimization is a rather common approach for producing aquaporins for structural characterization in microbial hosts like yeast and bacteria, exemplified by hAQP2 [15], hAQP10 [20], AtPIP2;4 [29] and PfAQP [33] **(Table 2)**.

Furthermore, worth reflecting on is whether high resolution structures are relevant determinants for successful protein production. The productions of SoPIP2;1 [61], hAQP1 [62] and hAQP10 [72] definitely point in this direction where high production levels were reported well in advance of the structure. Worth keeping in mind, as well, is that it is surprisingly difficult to compare yields of pure aquaporins from various production approaches and purifications; a systematic way to report yields is lacking meaning it is difficult to make proper comparisons between production trials even using the same system, and even less straight forward comparing systems with different cell densities. There is no consistency in the reporting of the yield; sometimes the final yield is reported and sometimes it is the yield after one purification step. Still, comparing reported yields for all structurally-determined aquaporins indicates that the apparent highest yield of a recombinant eukaryotic aquaporin is SoPIP2;1 produced in *P. pastoris* (25 mg/L) [60]. For a prokaryotic aquaporin, the highest yield achieved was for AqpZ, produced in *E. coli*, up to 13 mg/L [64]. This could be compared to even higher yields reported for hAQP1 recombinantly produced in *P. pastoris* where 90 mg/L was achieved after a two-step purification procedure [62] as well as 26.4 mg of affinity-purified hAQP10 from 50 g *S. cerevisiae* [72]. Overall, comparing the recombinant production of all aquaporins for which there is a high resolution structure, a consensus on

successful production emerges **(Fig. 5),** where the intrinsic benefit of using *P. pastoris* as host is the high cell mass achieved via fermenter growth [74].

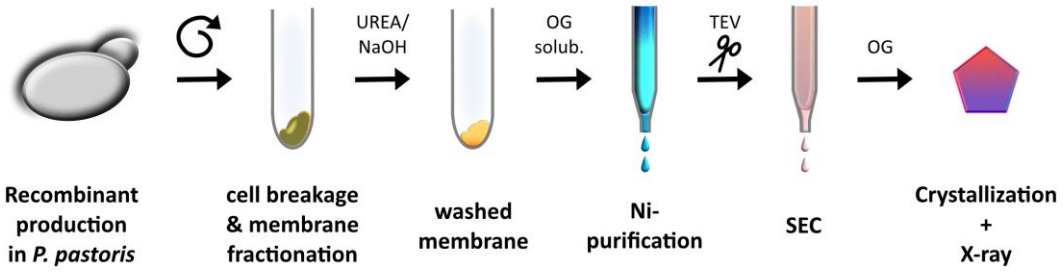

Figure 5. The most widely-used procedure for recombinant aquaporin production, purification and structural determination. Comparing all aquaporin structures determined to high resolution over the last 20 years, the most widely-used experimental strategy is recombinant production in *P. pastoris* (eukaryotic targets), membrane wash in urea followed by a wash in NaOH after cell breakage and fractionation, solubilization in OG, Ni-NTA purification, cleavage of the polyhistidine tag (if it is located in the N-terminus) using TEV-protease, a second purification step using size exclusion chromatography (SEC), possibly involving a detergent change, and finally preparation of crystals in OG for structural determination using X-ray crystallography.

Functionality is a critical assessment for purified proteins, especially so for integral membrane proteins where solubilization by detergents could be in conflict with proper folding and activity. In the beginning, functional data were not always included together with structural evaluation, but it is more or less standard in the more recent publications, sometimes also together with MD simulations and mutational analysis to shed light on molecular mechanisms. Evaluating aquaporin function using proteoliposomes is an accurate system in the sense that only one specific protein function is assayed at a time. Worth noting, however, is that it is difficult to compare functional data for purified aquaporins evaluated in different experiments, even for a specific aquaporin isoform. This is mainly due to the fact that there is no systematic way to specify activity as both initial rates, k, and the water permeability

constant, P_f, are reported. In addition, there are minor differences in the various setups used to measure function and, as a consequence, variations are reported for the same AQP isoform; exemplified by the initial rate measured for recombinant SoPIP2;1: k=10-15 s^{-1} [61] and 33.1±1.3 s^{-1} [62] where the applied lipid to protein ratio influences the measurement. A similar observation is made for recombinant AqpZ; k= 73,9 s^{-1} [38] and 102.9 s^{-1} [37]. Therefore, reliable comparisons ideally should be evaluated using the same settings in the same experimental setup. Furthermore, evaluation of proteoliposomes using stopped flow is a rather temperamental method where intrinsic variations in the preparations are difficult to avoid. It is therefore of major importance to include proper statistics when presenting the data which includes biological as well as technical repeats. Biological repeats must be done on reconstituted samples that use proteins from different purification trials and cultures, while technological repeats are replicate assays on the same reconstituted sample. In addition to that, averaged curves should be shown from each single technical repeat. Very seldom, however, such robust evaluation (with calculated standard deviations) is reported for aquaporin functional assessment.

Together with the power of genetic design, recombinant production also has the capacity to produce interesting mutants based on the structural evaluation, to be assessed *in vivo* or *in vitro*. The complication here is that both for cell based systems and reconstituted protein in liposomes, the actual protein amount could vary as a parameter linked to protein function and stability. As a consequence, the observed effect could be retrieved from different amounts of protein, something that has to be reflected on and adjusted for. This is not always taken into consideration, giving a high risk of misinterpretations of observed effects. A common practice, however, is to divide the measured velocities by estimated yields from SDS-PAGE gels or immunoblots which is a more accurate estimation of the actual velocity. Care has to be

taken, though, to ensure that the measured rate is within the linear range of the effect. Nevertheless, this aspect deserves to be reflected on when drawing conclusions based on comparisons of proteins, and ideally both real and adjusted data should be shown, as seen for mutational analysis of SoPIP2;1 [60].

Summarizing the findings in **Table 1** and **Fig. 5**, we note that the majority of aquaporin structures are determined by X-ray crystallography following crystallization of stable proteins in short chain detergents. Furthermore, as observed in **Table 2**, this commonly comes with the use of engineered proteins which are fused to tags for purification and are frequently truncated at their termini. It could be concluded that we have now established a concept for the production of individual aquaporins suitable for structural determination, and that we are now heading towards the understanding of function in a cellular context. However, aquaporin function includes regulation by proteins and protein complexes [48, 75], which commonly necessitates full length proteins for proper analysis. Related to this, methods including BiFC have been applied to keep low affinity aquaporin complexes together as a preparative step for structural evaluation [76]. Hence, it will be interesting to see what the development of EM will bring to the field. For example, a low-resolution structure of AQP0-CaM combined with MD and mutational analysis revealed the gating mechanism of AQP0 [77]. Furthermore, recent development in solid state NMR open up alternative methods of structural determination of membrane proteins and their complexes; the structure of hAQP1 is an exciting example of this [12]. Taken together, progress in recombinant production of aquaporins offers a framework for future insight into their regulatory mechanisms [44, 78-81] and cellular functions by combining structural evaluation and biochemical characterization.

4. Conclusions

Based on all high resolution structures achieved during the last 20 years, a consensus on how to produce high-quality samples of recombinant aquaporins has emerged. For a new aquaporin target, *E. coli* is a good choice to produce prokaryotic homologues and *P. pastoris* for those of eukaryotic origin. A cleavable N-terminal polyhistidine tag is recommended, and native sequence is preferred if yields are sufficient. OG most commonly works for solubilisation and purification using a two-step purification procedure: Ni-NTA affinity purification followed by SEC often results in high purity. Thus far, crystallization and X-ray crystallography have been the most successful approach for structural determination. It will be interesting to follow the development in membrane protein structure determination using ED and NMR and also the analysis of protein complexes in order to shed further light on regulatory mechanisms. Finally, a robust set of biological and technical repeats should be included in any functional evaluation using proteoliposomes assayed by stopped flow.

5. Acknowledgements

The work presented in this study was supported by research grants from the Swedish research Council (VR-M, Structural studies of aquaporin:protein complexes), VR-RÅC (2017-06727) and Brain Foundation (FO2018-0231) to Kristina Hedfalk and from the Biotechnology & Biosciences Research Council (through BB/P025927/1) to Roslyn Bill.

7. Author Contributions

Roslyn Bill Conceptualization, Formal analysis, Funding acquisition, Investigation, Project administration, Resources, Validation, Writing - review & editing.

Kristina Hedfalk Conceptualization, Data curation, Formal analysis, Funding acquisition, Investigation, Project administration, Resources, Validation, Writing - review & editing.

8. References

[1] E. Kruse, N. Uehlein, R. Kaldenhoff, The aquaporins, Genome Biol, 7 (2006) 206.
[2] D.E. Nordzieke, I. Medrano-Fernandez, The Plasma Membrane: A Platform for Intra- and Intercellular Redox Signaling, Antioxidants (Basel), 7 (2018).
[3] K. Ishibashi, S. Hara, S. Kondo, Aquaporin water channels in mammals, Clin Exp Nephrol, 13 (2009) 107-117.
[4] L. Tradtrantip, B.J. Jin, X. Yao, M.O. Anderson, A.S. Verkman, Aquaporin-Targeted Therapeutics: State-of-the-Field, Adv Exp Med Biol, 969 (2017) 239-250.
[5] S. Da Mesquita, A. Louveau, A. Vaccari, I. Smirnov, R.C. Cornelison, K.M. Kingsmore, C. Contarino, S. Onengut-Gumuscu, E. Farber, D. Raper, K.E. Viar, R.D. Powell, W. Baker, N. Dabhi, R. Bai, R. Cao, S. Hu, S.S. Rich, J.M. Munson, M.B. Lopes, C.C. Overall, S.T. Acton, J. Kipnis, Functional aspects of meningeal lymphatics in ageing and Alzheimer's disease, Nature, 560 (2018) 185-191.
[6] K. Stahl, S. Rahmani, A. Prydz, N. Skauli, N. MacAulay, M.N. Mylonakou, R. Torp, O. Skare, T. Berg, T.B. Leergaard, R.E. Paulsen, O.P. Ottersen, M. Amiry-Moghaddam, Targeted deletion of the aquaglyceroporin AQP9 is protective in a mouse model of Parkinson's disease, PLoS One, 13 (2018) e0194896.
[7] C. Maurel, Y. Boursiac, D.T. Luu, V. Santoni, Z. Shahzad, L. Verdoucq, Aquaporins in Plants, Physiol Rev, 95 (2015) 1321-1358.
[8] R. Kapilan, M. Vaziri, J.J. Zwiazek, Regulation of aquaporins in plants under stress, Biol Res, 51 (2018) 4.
[9] A. Tanghe, P. Van Dijck, J.M. Thevelein, Why do microorganisms have aquaporins?, Trends Microbiol, 14 (2006) 78-85.
[10] K. Murata, K. Mitsuoka, T. Hirai, T. Walz, P. Agre, J.B. Heymann, A. Engel, Y. Fujiyoshi, Structural determinants of water permeation through aquaporin-1, Nature, 407 (2000) 599-605.
[11] T. Walz, B.L. Smith, M.L. Zeidel, A. Engel, P. Agre, Biologically active two-dimensional crystals of aquaporin CHIP, J Biol Chem, 269 (1994) 1583-1586.
[12] D.A. Dingwell, L.S. Brown, V. Ladizhansky, Structure of the Functionally Important Extracellular Loop C of Human Aquaporin 1 Obtained by Solid-State NMR under Nearly Physiological Conditions, J Phys Chem B, 123 (2019) 7700-7710.
[13] G. Ren, V.S. Reddy, A. Cheng, P. Melnyk, A.K. Mitra, Visualization of a water-selective pore by electron crystallography in vitreous ice, Proc Natl Acad Sci U S A, 98 (2001) 1398-1403.
[14] D. Ruiz Carrillo, J. To Yiu Ying, D. Darwis, C.H. Soon, T. Cornvik, J. Torres, J. Lescar, Crystallization and preliminary crystallographic analysis of human aquaporin 1 at a resolution of 3.28 A, Acta Crystallogr F Struct Biol Commun, 70 (2014) 1657-1663.
[15] A. Frick, U.K. Eriksson, F. de Mattia, F. Oberg, K. Hedfalk, R. Neutze, W.J. de Grip, P.M. Deen, S. Tornroth-Horsefield, X-ray structure of human aquaporin 2 and its implications for nephrogenic diabetes insipidus and trafficking, Proceedings of the National Academy of Sciences of the United States of America, 111 (2014) 6305-6310.
[16] J. Lieske, M. Cerv, S. Kreida, D. Komadina, J. Fischer, M. Barthelmess, P. Fischer, T. Pakendorf, O. Yefanov, V. Mariani, T. Seine, B.H. Ross, E. Crosas, O. Lorbeer, A. Burkhardt, T.J. Lane, S. Guenther, J. Bergtholdt, S. Schoen, S. Tornroth-Horsefield, H.N. Chapman, A. Meents, On-chip crystallization for serial crystallography experiments and on-chip ligand-binding studies, IUCrJ, 6 (2019) 714-728.
[17] J.D. Ho, R. Yeh, A. Sandstrom, I. Chorny, W.E. Harries, R.A. Robbins, L.J. Miercke, R.M. Stroud, Crystal structure of human aquaporin 4 at 1.8 A and its mechanism of conductance, Proc Natl Acad Sci U S A, 106 (2009) 7437-7442.
[18] R. Horsefield, K. Norden, M. Fellert, A. Backmark, S. Tornroth-Horsefield, A.C. Terwisscha van Scheltinga, J. Kvassman, P. Kjellbom, U. Johanson, R. Neutze, High-resolution x-ray structure of human aquaporin 5, Proceedings of the National Academy of Sciences of the United States of America, 105 (2008) 13327-13332.
[19] S.W. de Mare, R. Venskutonyte, S. Eltschkner, B.L. de Groot, K. Lindkvist-Petersson, Structural Basis for Glycerol Efflux and Selectivity of Human Aquaporin 7, Structure, 28 (2020) 215-222 e213.

[20] K. Gotfryd, A.F. Mosca, J.W. Missel, S.F. Truelsen, K. Wang, M. Spulber, S. Krabbe, C. Helix-Nielsen, U. Laforenza, G. Soveral, P.A. Pedersen, P. Gourdon, Human adipose glycerol flux is regulated by a pH gate in AQP10, Nat Commun, 9 (2018) 4749.
[21] H. Sui, B.G. Han, J.K. Lee, P. Walian, B.K. Jap, Structural basis of water-specific transport through the AQP1 water channel, Nature, 414 (2001) 872-878.
[22] Y. Hiroaki, K. Tani, A. Kamegawa, N. Gyobu, K. Nishikawa, H. Suzuki, T. Walz, S. Sasaki, K. Mitsuoka, K. Kimura, A. Mizoguchi, Y. Fujiyoshi, Implications of the aquaporin-4 structure on array formation and cell adhesion, J Mol Biol, 355 (2006) 628-639.
[23] K. Tani, T. Mitsuma, Y. Hiroaki, A. Kamegawa, K. Nishikawa, Y. Tanimura, Y. Fujiyoshi, Mechanism of aquaporin-4's fast and highly selective water conduction and proton exclusion, J Mol Biol, 389 (2009) 694-706.
[24] T. Gonen, Y. Cheng, J. Kistler, T. Walz, Aquaporin-0 membrane junctions form upon proteolytic cleavage, Journal of molecular biology, 342 (2004) 1337-1345.
[25] T. Gonen, Y. Cheng, P. Sliz, Y. Hiroaki, Y. Fujiyoshi, S.C. Harrison, T. Walz, Lipid-protein interactions in double-layered two-dimensional AQP0 crystals, Nature, 438 (2005) 633-638.
[26] W.E. Harries, D. Akhavan, L.J. Miercke, S. Khademi, R.M. Stroud, The channel architecture of aquaporin 0 at a 2.2-A resolution, Proc Natl Acad Sci U S A, 101 (2004) 14045-14050.
[27] R.K. Hite, Z. Li, T. Walz, Principles of membrane protein interactions with annular lipids deduced from aquaporin-0 2D crystals, EMBO J, 29 (2010) 1652-1658.
[28] S. Tornroth-Horsefield, Y. Wang, K. Hedfalk, U. Johanson, M. Karlsson, E. Tajkhorshid, R. Neutze, P. Kjellbom, Structural mechanism of plant aquaporin gating, Nature, 439 (2006) 688-694.
[29] H. Wang, S. Schoebel, F. Schmitz, H. Dong, K. Hedfalk, Characterization of aquaporin-driven hydrogen peroxide transport, Biochim Biophys Acta Biomembr, 1862 (2020) 183065.
[30] A. Kirscht, S.S. Kaptan, G.P. Bienert, F. Chaumont, P. Nissen, B.L. de Groot, P. Kjellbom, P. Gourdon, U. Johanson, Crystal Structure of an Ammonia-Permeable Aquaporin, PLoS Biol, 14 (2016) e1002411.
[31] U.K. Eriksson, G. Fischer, R. Friemann, G. Enkavi, E. Tajkhorshid, R. Neutze, Subangstrom resolution X-ray structure details aquaporin-water interactions, Science, 340 (2013) 1346-1349.
[32] G. Fischer, U. Kosinska-Eriksson, C. Aponte-Santamaria, M. Palmgren, C. Geijer, K. Hedfalk, S. Hohmann, B.L. de Groot, R. Neutze, K. Lindkvist-Petersson, Crystal structure of a yeast aquaporin at 1.15 angstrom reveals a novel gating mechanism, PLoS biology, 7 (2009) e1000130.
[33] Z.E. Newby, J. O'Connell, 3rd, Y. Robles-Colmenares, S. Khademi, L.J. Miercke, R.M. Stroud, Crystal structure of the aquaglyceroporin PfAQP from the malarial parasite Plasmodium falciparum, Nat Struct Mol Biol, 15 (2008) 619-625.
[34] J.K. Lee, D. Kozono, J. Remis, Y. Kitagawa, P. Agre, R.M. Stroud, Structural basis for conductance by the archaeal aquaporin AqpM at 1.68 A, Proc Natl Acad Sci U S A, 102 (2005) 18932-18937.
[35] J. Jiang, B.V. Daniels, D. Fu, Crystal structure of AqpZ tetramer reveals two distinct Arg-189 conformations associated with water permeation through the narrowest constriction of the water-conducting channel, J Biol Chem, 281 (2006) 454-460.
[36] D.F. Savage, P.F. Egea, Y. Robles-Colmenares, J.D. O'Connell, 3rd, R.M. Stroud, Architecture and selectivity in aquaporins: 2.5 a X-ray structure of aquaporin Z, PLoS Biol, 1 (2003) E72.
[37] D.F. Savage, J.D. O'Connell, 3rd, L.J. Miercke, J. Finer-Moore, R.M. Stroud, Structural context shapes the aquaporin selectivity filter, Proc Natl Acad Sci U S A, 107 (2010) 17164-17169.
[38] D.F. Savage, R.M. Stroud, Structural basis of aquaporin inhibition by mercury, J Mol Biol, 368 (2007) 607-617.
[39] D. Fu, A. Libson, L.J. Miercke, C. Weitzman, P. Nollert, J. Krucinski, R.M. Stroud, Structure of a glycerol-conducting channel and the basis for its selectivity, Science, 290 (2000) 481-486.
[40] E. Tajkhorshid, P. Nollert, M.O. Jensen, L.J. Miercke, J. O'Connell, R.M. Stroud, K. Schulten, Control of the selectivity of the aquaporin water channel family by global orientational tuning, Science, 296 (2002) 525-530.
[41] S. Kreida, S. Tornroth-Horsefield, Structural insights into aquaporin selectivity and regulation, Curr Opin Struct Biol, 33 (2015) 126-134.
[42] T. Walz, T. Hirai, K. Murata, J.B. Heymann, K. Mitsuoka, Y. Fujiyoshi, B.L. Smith, P. Agre, A. Engel, The three-dimensional structure of aquaporin-1, Nature, 387 (1997) 624-627.

[43] J.S. Jung, G.M. Preston, B.L. Smith, W.B. Guggino, P. Agre, Molecular structure of the water channel through aquaporin CHIP. The hourglass model, J Biol Chem, 269 (1994) 14648-14654.
[44] V. Nesverova, S. Tornroth-Horsefield, Phosphorylation-Dependent Regulation of Mammalian Aquaporins, Cells, 8 (2019).
[45] S. Tornroth-Horsefield, K. Hedfalk, G. Fischer, K. Lindkvist-Petersson, R. Neutze, Structural insights into eukaryotic aquaporin regulation, FEBS Lett, 584 (2010) 2580-2588.
[46] R.E. Day, P. Kitchen, D.S. Owen, C. Bland, L. Marshall, A.C. Conner, R.M. Bill, M.T. Conner, Human aquaporins: regulators of transcellular water flow, Biochim Biophys Acta, 1840 (2014) 1492-1506.
[47] M. Zelenina, Regulation of brain aquaporins, Neurochemistry international, 57 (2010) 468-488.
[48] J.V. Roche, S. Tornroth-Horsefield, Aquaporin Protein-Protein Interactions, Int J Mol Sci, 18 (2017).
[49] J.D. Hoffert, R.A. Fenton, H.B. Moeller, B. Simons, D. Tchapyjnikov, B.W. McDill, M.J. Yu, T. Pisitkun, F. Chen, M.A. Knepper, Vasopressin-stimulated increase in phosphorylation at Ser269 potentiates plasma membrane retention of aquaporin-2, J Biol Chem, 283 (2008) 24617-24627.
[50] M.T. Conner, A.C. Conner, C.E. Bland, L.H. Taylor, J.E. Brown, H.R. Parri, R.M. Bill, Rapid aquaporin translocation regulates cellular water flow: mechanism of hypotonicity-induced subcellular localization of aquaporin 1 water channel, J Biol Chem, 287 (2012) 11516-11525.
[51] M.T. Conner, A.C. Conner, J.E. Brown, R.M. Bill, Membrane trafficking of aquaporin 1 is mediated by protein kinase C via microtubules and regulated by tonicity, Biochemistry, 49 (2010) 821-823.
[52] P. Kitchen, M.T. Conner, R.M. Bill, A.C. Conner, Structural Determinants of Oligomerization of the Aquaporin-4 Channel, J Biol Chem, 291 (2016) 6858-6871.
[53] P. Kitchen, R.E. Day, L.H. Taylor, M.M. Salman, R.M. Bill, M.T. Conner, A.C. Conner, Identification and Molecular Mechanisms of the Rapid Tonicity-induced Relocalization of the Aquaporin 4 Channel, J Biol Chem, 290 (2015) 16873-16881.
[54] P. Kitchen, M.M. Salman, A.M. Halsey, C. Clarke-Bland, J.A. MacDonald, H. Ishida, H.J. Vogel, S. Almutiri, A. Logan, S. Kreida, T. Al-Jubair, J. Winkel Missel, P. Gourdon, S. Tornroth-Horsefield, M.T. Conner, Z. Ahmed, A.C. Conner, R.M. Bill, Targeting Aquaporin-4 Subcellular Localization to Treat Central Nervous System Edema, Cell, 181 (2020) 784-799 e719.
[55] P. Kitchen, F. Oberg, J. Sjohamn, K. Hedfalk, R.M. Bill, A.C. Conner, M.T. Conner, S. Tornroth-Horsefield, Plasma Membrane Abundance of Human Aquaporin 5 Is Dynamically Regulated by Multiple Pathways, PLoS One, 10 (2015) e0143027.
[56] C.P. Kurtzman, Biotechnological strains of Komagataella (Pichia) pastoris are Komagataella phaffii as determined from multigene sequence analysis, J Ind Microbiol Biotechnol, 36 (2009) 1435-1438.
[57] D. Fotiadis, P. Jeno, T. Mini, S. Wirtz, S.A. Muller, L. Fraysse, P. Kjellbom, A. Engel, Structural characterization of two aquaporins isolated from native spinach leaf plasma membranes, J Biol Chem, 276 (2001) 1707-1714.
[58] A.N. van Hoek, M.C. Wiener, J.M. Verbavatz, D. Brown, P.H. Lipniunas, R.R. Townsend, A.S. Verkman, Purification and structure-function analysis of native, PNGase F-treated, and endo-beta-galactosidase-treated CHIP28 water channels, Biochemistry, 34 (1995) 2212-2219.
[59] P.J. Werten, L. Hasler, J.B. Koenderink, C.H. Klaassen, W.J. de Grip, A. Engel, P.M. Deen, Large-scale purification of functional recombinant human aquaporin-2, FEBS Lett, 504 (2001) 200-205.
[60] M. Nyblom, A. Frick, Y. Wang, M. Ekvall, K. Hallgren, K. Hedfalk, R. Neutze, E. Tajkhorshid, S. Tornroth-Horsefield, Structural and Functional Analysis of SoPIP2;1 Mutants Adds Insight into Plant Aquaporin Gating, Journal of Molecular Biology, 387 (2009) 653-668.
[61] M. Karlsson, D. Fotiadis, S. Sjovall, I. Johansson, K. Hedfalk, A. Engel, P. Kjellbom, Reconstitution of water channel function of an aquaporin overexpressed and purified from Pichia pastoris, FEBS Lett, 537 (2003) 68-72.
[62] M. Nyblom, F. Oberg, K. Lindkvist-Petersson, K. Hallgren, H. Findlay, J. Wikstrom, A. Karlsson, O. Hansson, P.J. Booth, R.M. Bill, R. Neutze, K. Hedfalk, Exceptional overproduction of a functional human membrane protein, Protein Expr Purif, 56 (2007) 110-120.
[63] M.J. Borgnia, D. Kozono, G. Calamita, P.C. Maloney, P. Agre, Functional reconstitution and characterization of AqpZ, the E. coli water channel protein, J Mol Biol, 291 (1999) 1169-1179.

[64] B.V. Daniels, J.S. Jiang, D. Fu, Crystallization and preliminary crystallographic analysis of the Escherichia coli water channel AqpZ, Acta Crystallogr D Biol Crystallogr, 60 (2004) 561-563.
[65] M.L. Zeidel, S.V. Ambudkar, B.L. Smith, P. Agre, Reconstitution of functional water channels in liposomes containing purified red cell CHIP28 protein, Biochemistry, 31 (1992) 7436-7440.
[66] G.M. Preston, J.S. Jung, W.B. Guggino, P. Agre, The mercury-sensitive residue at cysteine 189 in the CHIP28 water channel, J Biol Chem, 268 (1993) 17-20.
[67] R. Grisshammer, C.G. Tate, Overexpression of integral membrane proteins for structural studies, Q Rev Biophys, 28 (1995) 315-422.
[68] A. Kesidis, P. Depping, A. Lode, A. Vaitsopoulou, R.M. Bill, A.D. Goddard, A.J. Rothnie, Expression of eukaryotic membrane proteins in eukaryotic and prokaryotic hosts, Methods, 180 (2020) 3-18.
[69] C. Munk, E. Mutt, V. Isberg, L.F. Nikolajsen, J.M. Bibbe, T. Flock, M.A. Hanson, R.C. Stevens, X. Deupi, D.E. Gloriam, An online resource for GPCR structure determination and analysis, Nat Methods, 16 (2019) 151-162.
[70] J. Bomholt, C. Helix-Nielsen, P. Scharff-Poulsen, P.A. Pedersen, Recombinant production of human Aquaporin-1 to an exceptional high membrane density in Saccharomyces cerevisiae, PLoS One, 8 (2013) e56431.
[71] F. Oberg, M. Ekvall, M. Nyblom, A. Backmark, R. Neutze, K. Hedfalk, Insight into factors directing high production of eukaryotic membrane proteins; production of 13 human AQPs in Pichia pastoris, Molecular membrane biology, 26 (2009) 215-227.
[72] F.B. Bjorkskov, S.L. Krabbe, C.N. Nurup, J.W. Missel, M. Spulber, J. Bomholt, K. Molbaek, C. Helix-Nielsen, K. Gotfryd, P. Gourdon, P.A. Pedersen, Purification and functional comparison of nine human Aquaporins produced in Saccharomyces cerevisiae for the purpose of biophysical characterization, Sci Rep, 7 (2017) 16899.
[73] F. Oberg, K. Hedfalk, Recombinant production of the human aquaporins in the yeast Pichia pastoris (Invited Review), Molecular membrane biology, 30 (2013) 15-31.
[74] Z.E. Duman-Ozdamar, B. Binay, Production of Industrial Enzymes via Pichia pastoris as a Cell Factory in Bioreactor: Current Status and Future Aspects, Protein J, (2021).
[75] J. Sjohamn, K. Hedfalk, Unraveling aquaporin interaction partners, Biochimica et biophysica acta, 1840 (2014) 1614-1623.
[76] J. Sjohamn, P. Bath, R. Neutze, K. Hedfalk, Applying bimolecular fluorescence complementation to screen and purify aquaporin protein:protein complexes, Protein Sci, 25 (2016) 2196-2208.
[77] S.L. Reichow, D.M. Clemens, J.A. Freites, K.L. Nemeth-Cahalan, M. Heyden, D.J. Tobias, J.E. Hall, T. Gonen, Allosteric mechanism of water-channel gating by Ca-calmodulin, Nature structural & molecular biology, (2013).
[78] A. de Almeida, A.P. Martins, A.F. Mosca, H.J. Wijma, C. Prista, G. Soveral, A. Casini, Exploring the gating mechanisms of aquaporin-3: new clues for the design of inhibitors?, Mol Biosyst, 12 (2016) 1564-1573.
[79] L. Leitao, C. Prista, T.F. Moura, M.C. Loureiro-Dias, G. Soveral, Grapevine aquaporins: gating of a tonoplast intrinsic protein (TIP2;1) by cytosolic pH, PLoS One, 7 (2012) e33219.
[80] A.F. Mosca, A. de Almeida, D. Wragg, A.P. Martins, F. Sabir, S. Leoni, T.F. Moura, C. Prista, A. Casini, G. Soveral, Molecular Basis of Aquaporin-7 Permeability Regulation by pH, Cells, 7 (2018).
[81] F. Sabir, S. Gomes, M.C. Loureiro-Dias, G. Soveral, C. Prista, Molecular and Functional Characterization of Grapevine NIPs through Heterologous Expression in aqy-Null Saccharomyces cerevisiae, Int J Mol Sci, 21 (2020).